

A Microporous Metal–Organic Framework for Highly Selective Separation of Acetylene, Ethylene, and Ethane from Methane at Room Temperature

Yabing He,^[a] Zhangjing Zhang,^[a] Shengchang Xiang,^[a] Frank R. Fronczek,^[b] Rajamani Krishna,^{*[c]} and Banglin Chen^{*[a]}

Abstract: A novel three-dimensional microporous metal–organic framework $Zn_4L(DMA)_4$ (**UTSA-33**, $H_8L = 1,2,4,5$ -tetra(5-isophthalic acid)benzene, DMA = N,N' -dimethylacetamide) with small pores of about 4.8 to 6.5 Å was synthesized and structurally characterized as a non-interpenetrated (4,8)-connected network with the flu topology

(Schläfli symbol: $(4^{12}6^{12}8^4)(4^6)_2$). The activated **UTSA-33a** exhibits highly selective separation of acetylene, ethyl-

Keywords: breakthrough simulation • gas separation • hydrocarbons • microporous materials • metal–organic frameworks

ene, and ethane from methane with the adsorption selectivities of 12 to 20 at 296 K, which has been established exclusively by the sorption isotherms and simulated breakthrough experiments, thus methane can be readily separated from their binary and even ternary mixtures at room temperature.

Introduction

Separation of small hydrocarbons such as methane, acetylene, ethylene, and ethane is a very important industrial process because these small hydrocarbons have been widely utilized as energy sources and raw materials. Methane, the primary component of natural gas, is a cleaner alternative to other automobile fuels such as gasoline (petrol) and diesel; whereas ethane is the important chemical for the production of ethylene through industrial scale cracking processes. Both acetylene and ethylene are the very basic raw materials for various industrial and consumer products such as acetic acid, rubber and plastics. The traditional cryogenic distillation method for such small hydrocarbon separation is very energy-consuming, whereas the alternative oil-absorption method is not efficient. One of the most promising alternative energy- and cost-efficient separation methods is to use microporous adsorbents that can selectively separate methane from C_2 hydrocarbons at room temperature. It is envisioned that the realization of adsorptive separation of these

small hydrocarbons might lead to innovative technologies that will reduce the cost of removing C_2 hydrocarbons from natural gas feedstocks by the implementation of pressure swing adsorption (PSA), temperature swing adsorption (TSA) technologies, and/or adsorbent-based membrane devices. Porous metal–organic frameworks (MOFs), self-assembled from metal ions and/or metal-containing clusters with multidentate organic linkers through coordination bonding, have been rapidly emerging as a new type of microporous adsorbents and thus the unique sieving materials.^[1–14] The pores can be tuned by the organic linkers of different length and/or space, and the pore surfaces can be functionalized by the immobilization of functional sites, such as -NH₂ and -OH, into their isostructural MOFs.^[2,4,15] Thus, the MOF approach has theoretically enabled us to target microporous adsorbents with suitable pore sizes/curvatures and specific pore surfaces for the highly selective recognition, and therefore separation, of these small hydrocarbons, although not much research has been carried out.^[16] Given the fact that these hydrocarbons have kinetic diameters of 3.3 to 4.4 Å, those microporous MOFs for which the pores are comparable to and/or slightly larger than their kinetic diameters will be of special interest as the adsorbents for the separation of these small hydrocarbons. Previously, the construction of such small pores within porous MOFs has been mainly realized by framework interpenetration.^[14,16,17] In fact, we recently targeted the first microporous MOF $Zn_2(PBA)_2(BDC)$ (**UTSA-36a**, HPBA = 4-(4-pyridyl)benzoic acid, H₂BDC = 1,4-benzenedicarboxylic acid) of the doubly interpenetrated primitive cubic net with 3D-intersected pores of about 3.1 to 4.8 Å for the selective separation of C_2 from C_1 hydrocarbons.^[16] To rationalize the structure–property relationship and thus to maximize the C_2/C_1 separation selectivity and capacity, it is necessary to screen a variety of microporous MOFs of different pore

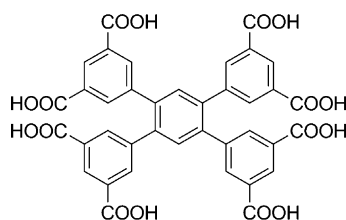
[a] Dr. Y. He, Dr. Z. Zhang, Dr. S. Xiang, Prof. Dr. B. Chen
Department of Chemistry, University of Texas at San Antonio
One UTSA Circle, San Antonio, Texas 78249-0698 (USA)
Fax: (+1) 210-458-7428
E-mail: banglin.chen@utsa.edu
Homepage: <http://www.utsa.edu/chem/chen.html>

[b] Dr. F. R. Fronczek
Department of Chemistry, Louisiana State University
Baton Rouge, LA 70803-1804 (USA)

[c] Prof. Dr. R. Krishna
Van 't Hoff Institute for Molecular Sciences,
University of Amsterdam Science Park 904
1098 XH Amsterdam (The Netherlands)
E-mail: r.krishna@uva.nl

 Supporting information for this article is available on the WWW under <http://dx.doi.org/10.1002/chem.201102734>.

structures and surface areas for such a function. However, enlarging the pores by the above-mentioned interpenetration methodology is basically crystallographically possible, but practically not feasible because longer organic linkers will typically lead to high-fold interpenetrated frameworks with even smaller pores or the same-fold interpenetrated frameworks with larger pores that cannot sustain vacuum and/or thermal activation.^[14,18] We have been developing new organic linkers (“organic-linker engineering”) to target MOFs with optimized and suitable pores (“pore engineering”) for gas storage and separation, which can be realized by different combinations of the organic backbones and the *m*-benzenedicarboxylate moieties.^[19] To enforce the construction of microporous MOFs with high stability and moderate pore sizes/curvatures, we develop a new organic linker H₈L (Scheme 1) with condensed *m*-benzenedicarboxylate



Scheme 1. The organic linker H₈L used to construct **UTSA-33**.

moieties. Herein, we report a novel microporous metal-organic framework Zn₄L(DMA)₄ (which we term as **UTSA-33**, H₈L=1,2,4,5-tetra(5-isophthalic acid)benzene, DMA=N,N'-dimethylacetamide) with small pores of about 4.8 to 6.5 Å for highly selective separation of acetylene, ethylene, and ethane from methane at room temperature, which has been established exclusively by the sorption isotherms and simulated breakthrough experiments.

Results and Discussion

The organic linker H₈L was synthesized by Pd-catalyzed Suzuki cross-coupling between 1,2,4,5-tetrabromobenzene and dimethyl 5-(pinacolboryl)isophthalate followed by base-catalyzed hydrolysis. **UTSA-33** was obtained as colorless block-shaped crystals by the solvothermal reaction of H₈L and Zn(NO₃)₂·6H₂O in N,N'-dimethylacetamide (DMA) at 100°C for 48 h. Its structure was determined by single-crystal X-ray diffraction,^[20] and the phase purity of the bulk material was confirmed by powder X-ray diffraction (PXRD) (Figure S1, see the Supporting Information). **UTSA-33** can be formulated as Zn₄L(DMA)₄ on the basis of single-crystal X-ray structure determination, thermogravimetric analysis (TGA), and microanalysis. TGA revealed a weight loss of 24.4% up to 300°C, corresponding to the release of the coordinated DMA solvent molecules (Figure S2 in the Supporting Information). Single-crystal X-ray diffraction analysis reveals **UTSA-33** adopts a 3D network that crystallizes

in an orthorhombic space group *Pnma*. The asymmetric unit consists of two zinc atoms, a half of a deprotonated ligand L and two terminal DMA molecules. Each organic linker contains four bridging carboxylates, two chelating ones and two chelating-bridging ones (Figure S3 in the Supporting Information). The secondary building unit (SBU) is a binuclear zinc-carboxylate cluster in which the Zn1 and Zn2 atoms are bridged by three carboxylate groups from three different ligands with a Zn1···Zn2 distance of 3.314(1) Å (Figure 1 a).

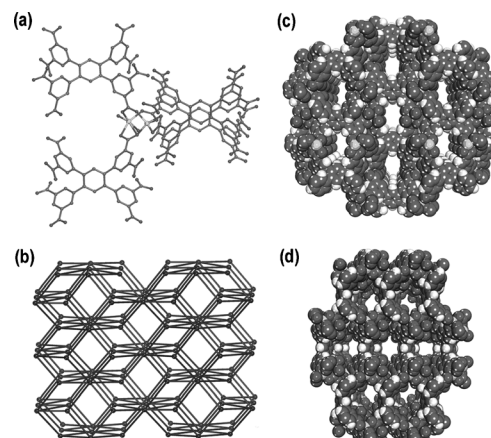


Figure 1. Single-crystal X-ray structure of **UTSA-33** indicating a) the binuclear zinc-carboxylate unit linked by four organic ligands, b) the flu topology, and c) and d) space-filling diagrams showing the channels along the *a* and *c* axes.

Besides, there are two terminal DMA molecules around Zn1 and a chelating carboxylate group around Zn2. Thus Zn1 and Zn2 adopt a six-coordinated and five-coordinated geometry, respectively. Topologically, each binuclear zinc-carboxylate cluster and each organic linker can be regarded as a 4-connected and 8-connected node, respectively, which are linked with each other to form a noninterpenetrated (4,8)-connected network with the flu topology (Schläfli symbol: (4¹²6¹²8⁴)(4⁶)₂) (Figure 1 b).^[21] There exist two types of micropores of approximately 5.4×6.5 Å along the *a* direction and 4.8×5.8 Å along the *c* direction, respectively, taking into account of the van der Waals radii (Figure 1 c and d). PLATON calculations indicate that **UTSA-33** contains 52.8% void space that is accessible to the solvent molecules after removal of coordinated DMA molecules from the Zn1 centers. To check the permanent porosity, the fresh sample was guest-exchanged with dry acetone and then activated under high vacuum at room temperature to generate the desolvated **UTSA-33a**. PXRD studies indicate that **UTSA-33a** still retains the crystalline feature (Figure S1 in the Supporting Information). The porosity was characterized by N₂ gas sorption at 77 K. The isotherm shows a Type-I sorption behavior typical for microporous materials with a Brunauer–Emmett–Teller (BET) and Langmuir surface area of 660.0 and 1024.3 m²g⁻¹, respectively, and a pore volume of 0.367 cm³g⁻¹ (Figure 2a and Figure S4 in the Supporting Information). The adsorbed amount is 237.4 cm³g⁻¹ (at stan-

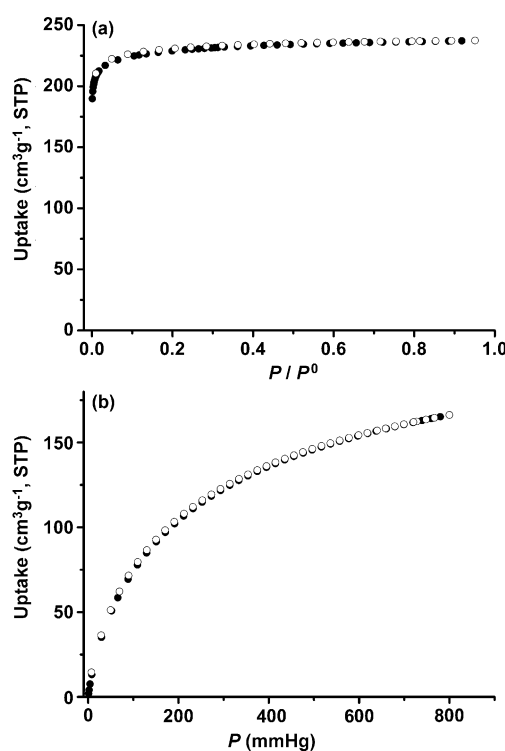


Figure 2. N₂ (a) and H₂ (b) sorption isotherms of **UTSA-33a** at 77 K. ●: adsorption, ○: desorption.

dard temperature and pressure (STP)) at $P/P^0=0.95$. The H₂ sorption isotherm at 77 K shows that **UTSA-33a** can adsorb H₂ to the amount of 166.3 cm³g⁻¹ (STP) (1.5 wt %) at 1 atm (Figure 2b). The hydrogen adsorption data follow closely the Langmuir–Freundlum equation ($R^2=0.99996$), from which the maximum adsorption of 237.6 cm³g⁻¹ (STP) (2.1 wt %) at 77 K can be predicted (Figure S5 in the Supporting Information). Establishment of the permanent porosity of **UTSA-33a** encouraged us to examine its potential application in gas separation, particularly for industrially important C₂/C₁ hydrocarbon separation. As shown in Figure 3, **UTSA-33a** exhibits different adsorption capacities to C₂H₂, C₂H₄, C₂H₆, and CH₄ at two different temperatures (273 and 296 K). The most remarkable and significant feature is that **UTSA-33a** systematically adsorbs many more C₂ hydrocarbons than C₁ methane. At 296 K, for example, **UTSA-33a** can take up a moderate amount of C₂H₂ (97.1 mg g⁻¹), C₂H₄ (76.2 mg g⁻¹), and C₂H₆ (83.0 mg g⁻¹), but basically a negligible amount of CH₄ (9.2 mg g⁻¹) at 1 atm (Figure 3a), thus highlighting **UTSA-33a** as a very promising material for highly selective adsorptive separation of C₂ hydrocarbons from CH₄ at room temperature. The separation selectivities, based on pure component molar loadings, of C₂H₂/CH₄, C₂H₄/CH₄, and C₂H₆/CH₄ at 296 K are 6.5, 4.7, and 4.8, respectively, which are systematically higher than those in our recently reported **UTSA-36a**.^[16] Using the dual-Langmuir fits of pure component isotherms (Figures S6–S9 in the Supporting Information), the adsorption selectivities, S_{ads} , are defined by the following equation:

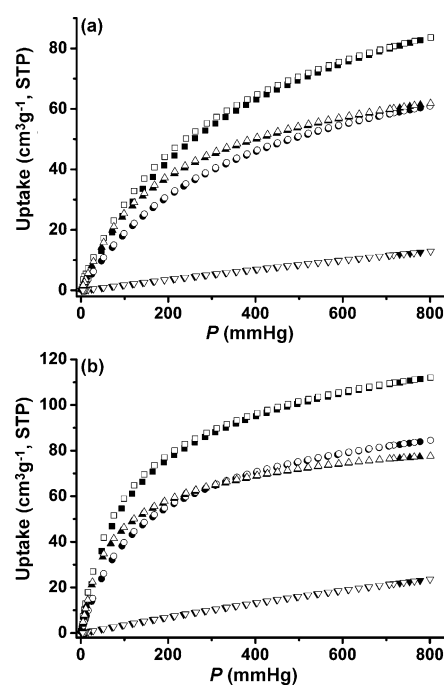


Figure 3. C₂H₂ (■ and □), C₂H₄ (● and ○), C₂H₆ (▲ and △), and CH₄ (▼ and ▽) sorption isotherms of **UTSA-33a** at a) 296 K and b) 273 K. Solid symbols: adsorption, open symbols: desorption.

$$S_{ads} = \frac{q_1/q_2}{p_1/p_2} \quad (1)$$

in which p_i the bulk gas pressure of species i , and q_i the component molar loading of species i , can be determined using the ideal adsorbed solution theory (IAST) of Myers and Prausnitz.^[22] The accuracy of IAST for estimation of binary mixture equilibrium in zeolites and MOFs has been established in a number of publications in the literature.^[23] Figure 4 shows the IAST calculations of the adsorption selectivity, S_{ads} , for equimolar C₂H₂/CH₄, C₂H₄/CH₄, and C₂H₆/CH₄ mixtures at 296 K in **UTSA-33a**. The selectivities of C₂H₄ with respect to CH₄ are in excess of 12 for a range of

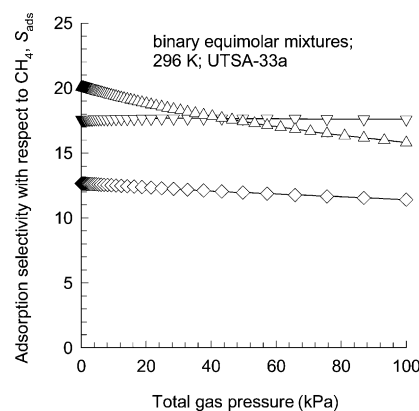


Figure 4. Calculations of the adsorption selectivity, S_{ads} , for equimolar C₂H₂/CH₄ (▽), C₂H₄/CH₄ (◇), and C₂H₆/CH₄ (△) mixtures at 296 K in **UTSA-33a** using IAST.

pressures to 100 kPa; separation of this binary mixture is therefore expected to be easy. For $\text{C}_2\text{H}_2/\text{CH}_4$ and $\text{C}_2\text{H}_6/\text{CH}_4$ mixtures, the adsorption selectivities are in excess of 16, and thus separations of these binary mixtures are even easier.

To understand such high separation selectivity, the isosteric heat of adsorption, Q_{st} , defined as

$$Q_{st} = RT^2 \left(\frac{\partial \ln p}{\partial T} \right)_q \quad (2)$$

was determined by using the pure component isotherm fit (Figures S6–S9 in the Supporting Information). Figure 5 presents the data on the isosteric heats of adsorption for

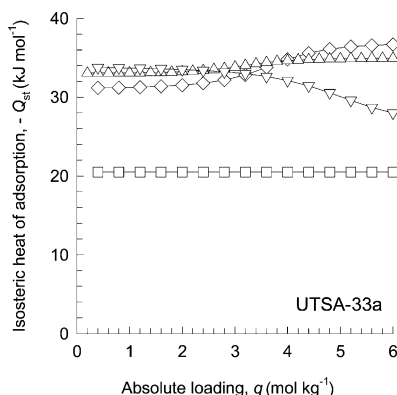


Figure 5. The isosteric heats of adsorption for C_2H_2 (∇), C_2H_4 (\diamond), C_2H_6 (\triangle), and CH_4 (\square) in **UTSA-33a**.

C_2H_2 , C_2H_4 , C_2H_6 , and CH_4 in **UTSA-33a**. These calculations are based on the use of equation (2), along with analytic differentiation of the isotherm fits of the dual-Langmuir fit parameters provided in Tables S1–S4 (see the Supporting Information). The analytic procedure used is identical to the one described in detail in the Supplementary Information accompanying the paper by Mason et al.^[24] The isosteric heat of adsorption of CH_4 in **UTSA-33a** is significantly lower, and has a value of 20.5 kJ mol^{-1} , whereas the isosteric heats of adsorption of C_2H_2 , C_2H_4 , and C_2H_6 are close to one another, and have a value of about 32 kJ mol^{-1} in the limit of low loadings. The higher adsorption heats for C_2 hydrocarbons might be due to the comparable pore sizes in **UTSA-33a** with these small C_2 hydrocarbons, thereby enforcing their interaction with the host framework, and thus leading to highly selective separation of C_2 over C_1 hydrocarbons.

The separation characteristic of any adsorbent is dictated not only by the adsorption selectivity, but also by the adsorption capacity. The appropriate combination of the selectivity and capacity characteristics is reflected in the breakthrough behavior in a packed-bed adsorber. Figure 6 (top) shows a schematic of a packed bed adsorber. The breakthrough characteristics were simulated using the methodology described in the work of Krishna and Long.^[25] Assuming

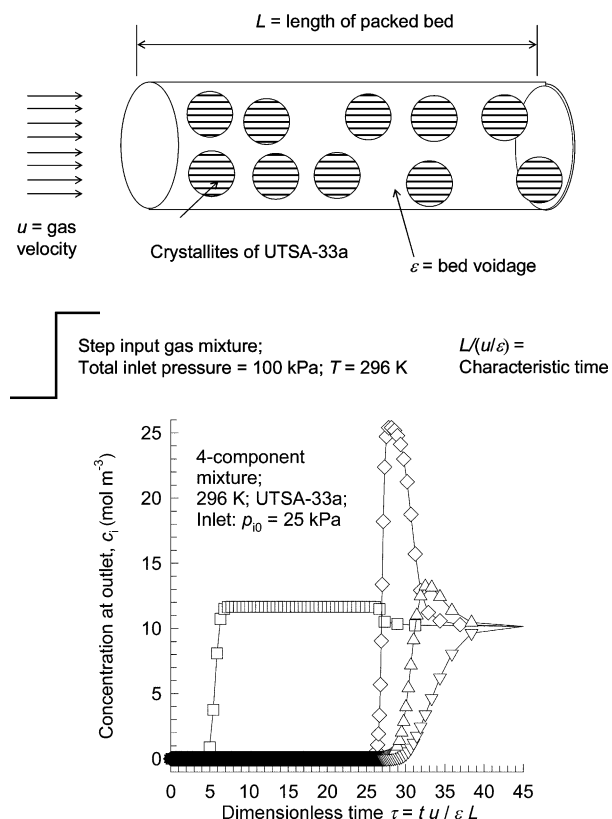


Figure 6. Schematic of packed-bed adsorber (top) and transient breakthrough of an equimolar 4-component mixture containing C_2H_2 (∇), C_2H_4 (\diamond), C_2H_6 (\triangle), and CH_4 (\square) in adsorber packed with **UTSA-33a**, operating at isothermal conditions at 296 K. The inlet gas is maintained at partial pressures $p_{i0} = 25 \text{ kPa}$. Video animations showing the motion of gas phase concentration fronts traversing the length of the adsorber with the 4-component mixture have been provided as Supporting Information.

isothermal conditions, with the adsorber maintained at 296 K, the transient breakthrough of an equimolar 4-component mixture of C_2H_2 , C_2H_4 , C_2H_6 , and CH_4 at 296 K in **UTSA-33a** were determined. The molar concentrations of the gas phase exiting the adsorber are shown in Figure 6 (bottom) for a gas mixture with partial pressures of 25 kPa each for each of the four components at the inlet. The x -axis is a dimensionless time, τ , obtained by dividing the actual time, t , by the contact time between the gas and the crystallites, $\varepsilon L/u$. For a given adsorbent, under chosen operating conditions, the breakthrough characteristics are uniquely defined by τ , allowing the results to be presented here to be equally applicable to laboratory scale equipment, as well as to industrial scale adsorbers. Specifically, the calculations presented here were performed taking the following parameter values: $L = 0.12 \text{ m}$; $\varepsilon = 0.75$; $u = 0.00225 \text{ m s}^{-1}$. The framework density of **UTSA-33a** is 993 kg m^{-3} . From the breakthrough curves presented in Figure 6 (right), we note that CH_4 , the component with the poorest adsorption strength “breaks through” earliest and it is possible to produce pure methane from this 4-component mixture during the adsorption cycle. The feasibility of separation of CH_4

from mixtures containing C₂H₂, C₂H₄, or C₂H₆ is also emphasized by determining the breakthrough characteristics of binary mixtures C₂H₂/CH₄, C₂H₄/CH₄, and C₂H₆/CH₄ at 296 K (Figures S10–S12 A in the Supporting Information). For each of these three mixtures, there is a significant gap between the breakthroughs of CH₄ and the partner species. This further indicates the feasibility of recovering pure CH₄ during the adsorption phase. After the adsorption cycle is complete, the component that is preferentially adsorbed, C₂H₂, C₂H₄, or C₂H₆, can be recovered by purging. The desorption characteristics using an inert, non-adsorbing gas are shown in Figures S10–S12 B (in the Supporting Information). It is clear that pure C₂H₂, C₂H₄, or C₂H₆ can be recovered from the purge gas. The breakthrough calculations confirm the potency of **UTSA-33a** in separating CH₄ from mixtures containing one or more of the species C₂H₂, C₂H₄, and C₂H₆.

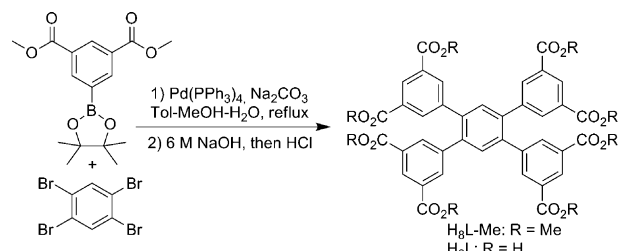
Conclusion

We have successfully realized a novel moderately porous microporous metal-organic framework for highly selective separation of C₂ hydrocarbons from C₁ methane at room temperature. This new MOF exhibits not only higher adsorption capacity, but also higher separation selectivities than the previously established **UTSA-36a**, indicating the feasibility to tune the pore structures and/or surfaces within porous MOF materials for the enhanced C₂/C₁ separation. This work will initiate more extensive research on this important subject and some practically useful microporous MOF materials will be targeted and eventually implemented into these industrially important separations in the future.

Experimental Section

Materials and measurements: All reagents and solvents were used as received from commercial suppliers without further purification. ¹H NMR and ¹³C NMR spectra were recorded on Varian Mercury 300 MHz or Bruker AV600 spectrometer. Tetramethylsilane (TMS) and deuterated solvents (CDCl₃, δ = 77.0 ppm; [D₆]DMSO, δ = 39.5 ppm) were used as internal standards in ¹H NMR and ¹³C NMR experiments, respectively. The coupling constants were reported in Hertz. FTIR spectra were performed on a Bruker Vector 22 spectrometer at room temperature. The elemental analyses were performed with Perkin-Elmer 240 CHN analyzers from Galbraith Laboratories, Knoxville. Thermogravimetric analyses (TGA) were measured using a Shimadzu TGA-50 analyzer under a nitrogen atmosphere with a heating rate of 3 °C min⁻¹. Powder X-ray diffraction (PXRD) patterns were recorded by a Rigaku Ultima IV diffractometer operated at 40 kV and 44 mA with a scan rate of 1.0 deg min⁻¹. A Micromeritics ASAP 2020 surface area analyzer was used to measure gas adsorption isotherms. To remove the guest solvent molecules in the framework, the fresh sample was exchanged with dry acetone at least 5 times, filtered and vacuumed at room temperature until the outgas rate was 5 μHg min⁻¹ prior to measurements. A sample of 125.4 mg was used for the sorption measurement and was maintained at 77 K with liquid nitrogen and at 273 K with an ice-water bath. As the center-controlled air condition was set up at 23 °C, a water bath was used for adsorption isotherms at 296 K.

Synthesis and characterization of the organic linker H₈L: The synthetic route to the organic linker H₈L was shown in Scheme 2.



Scheme 2. The synthetic route to the organic linker H₈L.

1,2,4,5-tetra(3,5-dimethoxycarboxyphenyl)benzene (H₈L-Me): The degassed mixed solvents (toluene/MeOH/H₂O, 120:60:60 mL) were added to a mixture of 1,2,4,5-tetrabromobenzene (2.50 g, 6.35 mmol), dimethyl 5-(pinacolboryl)isophthalate (12.20 g, 38.11 mmol), Na₂CO₃ (10.77 g, 101.61 mmol), and Pd(PPh₃)₄ (1.47 g, 1.27 mmol) under a nitrogen atmosphere. The resulting mixture was stirred for 72 h under reflux. After removal of the solvent, the residue was extracted with dichloromethane (80 × 3 mL), washed with brine (80 mL), dried over anhydrous MgSO₄, filtered, and concentrated in vacuo. The residue was purified by silica gel column chromatography to give 1,2,4,5-tetra(3,5-dimethoxycarboxyphenyl)benzene as a pure white solid (4.14 g, 4.89 mmol, 77% yield). ¹H NMR (CDCl₃, 300.0 MHz) δ = 8.55 (t, J = 1.5 Hz, 4H), 8.061 (d, J = 1.5 Hz, 8H), 7.58 (s, 2H), 3.89 ppm (s, 24H); ¹³C NMR (CDCl₃, 75.4 MHz) δ = 165.57, 140.26, 138.76, 134.76, 132.66, 130.64, 129.46, 52.48 ppm; FTIR ν = 2952, 1718, 1599, 1430, 1331, 1298, 1236, 1126, 1107, 1072, 997, 963, 907, 875, 832, 786, 769, 753, 721, 692 cm⁻¹.

1,2,4,5-tetra(5-isophthalic acid)benzene (H₈L): A 6 M aqueous solution of NaOH (60 mL, 360 mmol) was added to a solution of 1,2,4,5-tetra(3,5-dimethoxycarboxyl)benzene (4.50 g, 5.31 mmol) in methanol (150 mL). The resulting mixture was stirred under reflux overnight. After removal of the solvent, the residue was dissolved in H₂O and filtered. The filtrate was neutralized with concentrated HCl at 0 °C. The resulting precipitate was collected by filtration, washed with H₂O and dried in vacuo at 80 °C to afford the target compound as an off-white solid (3.85 g, 5.24 mmol) in 99% yield. ¹H NMR ([D₆]DMSO, 600.1 MHz) δ = 13.20 (brs, 8H), 8.35 (t, J = 1.2 Hz, 4H), 8.00 (d, J = 1.2 Hz, 8H), 7.78 ppm (s, 2H); ¹³C NMR ([D₆]DMSO, 150.9 MHz) δ = 166.19, 140.18, 138.38, 134.50, 132.62, 131.35, 128.67 ppm; FTIR ν = 1685, 1597, 1439, 1392, 1193, 1137, 1000, 906, 751, 704, 658 cm⁻¹.

Synthesis and characterization of UTSA-33: A mixture of the organic linker H₈L (10.0 mg, 13.6 mmol) and Zn(NO₃)₂·6H₂O (20.0 mg, 67.2 mmol) was dissolved into N,N'-dimethylacetamide (DMA, 1.5 mL) in a screw-capped vial (20 mL). The vial was then capped and heated at 100 °C for 48 h. The colorless block-shaped crystals were collected in 65% yield. **UTSA-33** can be formulated as Zn₄L(DMA)₄ on the basis of single-crystal X-ray structure determination, TGA, and microanalysis. FTIR ν = 1600, 1583, 1507, 1399, 1351, 1257, 1190, 1106, 1060, 1018, 964, 919, 851, 778, 744, 720, 682 cm⁻¹; TGA data: calcd (%) weight loss for 4DMA: 26.0; found: 24.4; elemental analysis calcd (%) for C₅₄H₅₀N₄O₂₀Zn₄: C 48.53, H 3.77, N 4.19; found: C 48.37, H 3.81, N 4.23.

Single-crystal X-ray structure determination: Crystal data for the reported **UTSA-33** were collected at 90 K on a Bruker SMART Apex II CCD-based X-ray diffractometer system equipped with a Cu-target X-ray tube (λ = 1.54178 Å) operated at 2000 watts power (50 kV, 40 mA). The structure was solved by direct methods and refined to convergence by the least squares method on F² using the SHELXTL software suit.^[26] The hydrogen atoms on the ligands were placed in idealized positions and refined using a riding model. The DMA solvents could not be located. We employed PLATON/SQUEEZE to calculate the diffraction contribution of the solvent molecules and thereby produce a set of solvent-free diffraction intensities. CCDC-837371 (**UTSA-33**) contains the supplementary crystallographic data for this paper. These data can be obtained free of charge from The Cambridge Crystallographic Data Centre via www.ccdc.cam.ac.uk/data_request/cif.

Acknowledgements

This work was supported by an award AX-1730 from the Welch Foundation (BC).

- [1] a) O. M. Yaghi, M. O'Keeffe, N. W. Ockwig, H. K. Chae, M. Eddaoudi, J. Kim, *Nature* **2003**, *423*, 705–714; b) S. Kitagawa, R. Kitaura, S. I. Noro, *Angew. Chem.* **2004**, *116*, 2388–2430; *Angew. Chem. Int. Ed.* **2004**, *43*, 2334–2375; c) G. Férey, C. Mellot-Draznin, C. Serre, F. Millange, *Acc. Chem. Res.* **2005**, *38*, 217–225; d) R. E. Morris, P. S. Wheatley, *Angew. Chem.* **2008**, *120*, 5044–5059; *Angew. Chem. Int. Ed.* **2008**, *47*, 4966–4981; e) J. Li, R. J. Kuppler, H.-C. Zhou, *Chem. Soc. Rev.* **2009**, *38*, 1477–1504; f) L. J. Murray, M. Dinca, J. R. Long, *Chem. Soc. Rev.* **2009**, *38*, 1294–1314; g) S. Ma, H.-C. Zhou, *Chem. Commun.* **2010**, *46*, 44; h) X. Lin, N. R. Champness, M. Schröder, *Top. Curr. Chem.* **2010**, *293*, 35–76; i) H.-L. Jiang, Q. Xu, *Chem. Commun.* **2011**, *47*, 3351–3370; j) B. Chen, S. C. Xiang, G. Qian, *Acc. Chem. Res.* **2010**, *43*, 1115–1124; k) Z. Zhang, S. Xiang, B. Chen, *CrystEngComm* **2011**, DOI:10.1039/c1ce05437f; l) W. Zhou, *Chem. Rec.* **2010**, *10*, 200–204.
- [2] M. Eddaoudi, J. Kim, N. Rosi, D. Vodak, J. Wachter, M. O'Keeffe, O. M. Yaghi, *Science* **2002**, *295*, 469–472.
- [3] a) S. C. Xiang, W. Zhou, J. M. Gallegos, Y. Liu, B. Chen, *J. Am. Chem. Soc.* **2009**, *131*, 12415–12419; b) H. Wu, W. Zhou, T. Yildirim, *J. Am. Chem. Soc.* **2009**, *131*, 4995–5000; c) S. C. Xiang, W. Zhou, Z. J. Zhang, M. A. Green, Y. Liu, B. Chen, *Angew. Chem.* **2010**, *122*, 4719–4722; *Angew. Chem. Int. Ed.* **2010**, *49*, 4615–4618; d) H. Wu, J. M. Simmons, Y. Liu, C. M. Brown, X.-S. Wang, S. Ma, V. K. Peterson, P. D. Southon, C. J. Kepert, H.-C. Zhou, T. Yildirim and W. Zhou, *Chem. Eur. J.* **2010**, *16*, 5205–5214.
- [4] a) R. Vaidhyanathan, S. S. Iremonger, K. W. Dawson, G. K. H. Shimizu, *Chem. Commun.* **2009**, 5230–5232; b) R. Vaidhyanathan, S. S. Iremonger, G. K. H. Shimizu, P. G. Boyd, S. Alavi, T. K. Woo, *Science* **2010**, *330*, 650–653.
- [5] a) T. K. Maji, K. Uemura, H.-C. Chang, R. Matsuda, S. Kitagawa, *Angew. Chem.* **2004**, *116*, 3331–3334; *Angew. Chem. Int. Ed.* **2004**, *43*, 3269–3272; b) S. Horike, S. Shimomura, S. Kitagawa, *Nat. Chem.* **2009**, *1*, 695–704.
- [6] a) S. Ma, D. Sun, X. S. Wang, H.-C. Zhou, *Angew. Chem.* **2007**, *119*, 2510–2514; *Angew. Chem. Int. Ed.* **2007**, *46*, 2458–2462; b) S. Ma, D. Sun, D. Yuan, X. S. Wang, H.-C. Zhou, *J. Am. Chem. Soc.* **2009**, *131*, 6445–6451.
- [7] a) J.-P. Zhang, X.-M. Chen, *J. Am. Chem. Soc.* **2009**, *131*, 5516–5521; b) J.-P. Zhang, X.-M. Chen, *J. Am. Chem. Soc.* **2008**, *130*, 6010–6017.
- [8] a) S.-T. Zheng, J. T. Bu, Y. Li, T. Wu, F. Zuo, P. Feng, X. Bu, *J. Am. Chem. Soc.* **2010**, *132*, 17062–17064; b) S. Zheng, Y. Li, T. Wu, R. Nieto, P. Feng, X. Bu, *Chem. Eur. J.* **2010**, *16*, 13035–13040; c) S. Chen, J. Zhang, T. Wu, P. Feng, X. Bu, *J. Am. Chem. Soc.* **2009**, *131*, 16027–16029.
- [9] a) I. Imaz, M. R.-M. nez, J. An, I. S. -Font, N. L. Rosi and D. Maspoch, *Chem. Commun.* **2011**, *47*, 7287–7302; b) J. An, R. P. Fiorella, S. J. Geib, N. L. Rosi, *J. Am. Chem. Soc.* **2009**, *131*, 8401–8403; c) J. An, S. J. Geib, N. L. Rosi, *J. Am. Chem. Soc.* **2010**, *132*, 38–39.
- [10] a) L. Pan, B. Parker, X. Huang, D. H. Olson, J. Lee, J. Li, *J. Am. Chem. Soc.* **2006**, *128*, 4180–4181; b) L. Pan, D. H. Olson, L. R. Ciernolonski, R. Heddy, J. Li, *Angew. Chem.* **2006**, *118*, 632–635; *Angew. Chem. Int. Ed.* **2006**, *45*, 616–619; c) K. Li, D. H. Olson, J. Seidel, T. J. Emge, H. Gong, H. Zeng, J. Li, *J. Am. Chem. Soc.* **2009**, *131*, 10368–10369; d) H. Wu, R. S. Reali, D. A. Smith, M. C. Trachtenberg and J. Li, *Chem. Eur. J.* **2010**, *16*, 13951–13954; e) Y. Zhao, H. Wu, T. J. Emge, Q. Gong, N. Nijem, Y. J. Chabal, L. Kong, D. C. Langreth, H. Liu, H. Zeng and J. Li, *Chem. Eur. J.* **2011**, *17*, 5101–5109.
- [11] a) Z. Xin, J. Bai, Y. Pan, M. J. Zaworotko, *Chem. Eur. J.* **2010**, *16*, 13049–13052; b) B. Zheng, J. Bai, J. Duan, L. Wojtas, M. J. Zaworotko, *J. Am. Chem. Soc.* **2011**, *133*, 748–751.
- [12] a) M. C. Das, P. K. Bharadwaj, *J. Am. Chem. Soc.* **2009**, *131*, 10942–10949; b) M. K. Sharma, I. Senkovska, S. Kaskel, P. K. Bharadwaj, *Inorg. Chem.* **2011**, *50*, 539–544; c) P. Lama, A. Ajaz, S. Neogi, L. J. Barbour and P. K. Bharadwaj, *Cryst. Growth Des.* **2010**, *10*, 3410–3417.
- [13] a) D. Britt, H. Furukawa, B. Wang, T. G. Glover, O. M. Yaghi, *Proc. Natl. Acad. Sci. USA* **2009**, *106*, 20637–20640; b) C. Güçüyener, J. van den Bergh, J. Gascon, F. Kapteijn, *J. Am. Chem. Soc.* **2010**, *132*, 17704–17706; c) S. M. Humphrey, J.-S. Chang, S. H. Jhung, J. W. Yoon, P. T. Wood, *Angew. Chem.* **2007**, *119*, 276–279; *Angew. Chem. Int. Ed.* **2007**, *46*, 272–275; d) D. N. Dybtsev, H. Chun, S. H. Yoon, D. Kim, K. Kim, *J. Am. Chem. Soc.* **2004**, *126*, 32–33; e) J.-R. Li, Y. Tao, Q. Yu, Z.-H. Bu, H. Sakamoto, S. Kitagawa, *Chem. Eur. J.* **2008**, *14*, 2771–2776; f) M. Dinca, J. R. Long, *J. Am. Chem. Soc.* **2005**, *127*, 9376–9377; g) Y. E. Cheon, M. P. Suh, *Chem. Commun.* **2009**, 2296–2298; h) S. Couck, J. F. M. Denayer, G. V. Baron, T. Rémy, J. Gascon, F. Kapteijn, *J. Am. Chem. Soc.* **2009**, *131*, 6326–6327; i) Z. Zhang, S. Xiang, Y.-S. Chen, S. Ma, Y. Lee, T. Phely-Bobin, B. Chen, *Inorg. Chem.* **2010**, *49*, 8444–8448; j) L. Bastin, P. S. Barcia, E. J. Hurtado, J. A. C. Silva, A. E. Rodrigues, B. Chen, *J. Phys. Chem. C* **2008**, *112*, 1575–1581; k) T. K. Maji, R. Matsuda, S. Kitagawa, *Nat. Mater.* **2007**, *6*, 142–148; l) E.-Y. Choi, K. Park, C.-M. Yang, H. Kim, J.-H. Son, S. W. Lee, Y. H. Lee, D. Min, Y.-U. Kwon, *Chem. Eur. J.* **2004**, *10*, 5535–5540; m) S. Xiang, Z. Zhang, C.-G. Zhao, K. Hong, X. Zhao, D.-R. Ding, M.-H. Xie, C.-D. Wu, M. C. Das, R. Gill, K. M. Thomas, B. Chen, *Nat. Commun.* **2011**, *2*, 204; n) P. K. Thallapally, J. Tian, M. R. Kishan, C. A. Fernandez, S. J. Dalgarno, P. B. McGrail, J. E. Warren, J. L. Atwood, *J. Am. Chem. Soc.* **2008**, *130*, 16842–16843; o) E. D. Bloch, L. J. Murray, W. L. Queen, S. Chavan, S. N. Maximoff, J. P. Bigi, R. Krishna, V. K. Peterson, F. Grandjean, G. J. Long, B. Smit, S. Bordiga, C. M. Brown and J. R. Long, *J. Am. Chem. Soc.* **2011**, *133*, 14814–14822; p) T. Panda, P. Pachfule, Y. Chen, J. Jiang, R. Banerjee, *Chem. Commun.* **2011**, *47*, 2011–2013; q) S. R. Caskey, A. G. Wong-Foy, A. J. Matzger, *J. Am. Chem. Soc.* **2008**, *130*, 10870–10871; r) S.-S. Chen, M. Chen, S. Takamizawa, P. Wang, G.-C. Lv, W.-Y. Sun, *Chem. Commun.* **2011**, *47*, 4902–4904; s) F. Wang, Y.-X. Tan, H. Yang, H.-X. Zhang, Y. Kang, J. Zhang, *Chem. Commun.* **2011**, *47*, 5828–5830; t) K. Gedrich, I. Senkovska, N. Klein, U. Stoeck, A. Henschel, M. R. Lohe, I. A. Baburin, U. Mueller, S. Kaskel, *Angew. Chem.* **2010**, *122*, 8667–8670; *Angew. Chem. Int. Ed.* **2010**, *49*, 8489–8492; u) Y. Ling, Z.-X. Chen, F.-P. Zhai, Y.-M. Zhou, L.-H. Weng, D.-Y. Zhao, *Chem. Commun.* **2011**, *47*, 7197–7199; v) D.-C. Zhong, W.-X. Zhang, F.-L. Cao, L. Jiang, T.-B. Lu, *Chem. Commun.* **2011**, *47*, 1204–1206.
- [14] a) B. Chen, C. Liang, J. Yang, D. S. Contreras, Y. L. Clancy, E. B. Lobkovsky, O. M. Yaghi, S. Dai, *Angew. Chem.* **2006**, *118*, 1418–1421; *Angew. Chem. Int. Ed.* **2006**, *45*, 1390–1393; b) B. Chen, S. Ma, F. Zapata, E. B. Lobkovsky, J. Yang, *Inorg. Chem.* **2006**, *45*, 5718–5720; c) P. S. Bárbara, F. Zapata, J. A. C. Silva, A. E. Rodrigues, B. Chen, *J. Phys. Chem. B* **2007**, *111*, 6101–6103; d) B. Chen, S. Ma, F. Zapata, F. R. Fronczeck, E. B. Lobkovsky, H.-C. Zhou, *Inorg. Chem.* **2007**, *46*, 1233–1236; e) B. Chen, S. Ma, E. J. Hurtado, E. B. Lobkovsky, H.-C. Zhou, *Inorg. Chem.* **2007**, *46*, 8490–8492; f) B. Chen, S. Ma, E. J. Hurtado, E. B. Lobkovsky, C. Liang, H. Zhu, S. Dai, *Inorg. Chem.* **2007**, *46*, 8705–8709.
- [15] a) Z. Chen, S. Xiang, H. D. Arman, P. Li, D. Zhao, B. Chen, *Eur. J. Inorg. Chem.* **2010**, 3745; b) Z. Chen, S. Xiang, H. D. Arman, J. U. Mondal, P. Li, D. Zhao, B. Chen, *Inorg. Chem.* **2011**, *50*, 3442; c) Z. Chen, S. Xiang, H. D. Arman, P. Li, D. Zhao, B. Chen, *Eur. J. Inorg. Chem.* **2011**, 2227.
- [16] M. C. Das, H. Xu, S. Xiang, Z. Zhang, H. D. Arman, G. Qian and B. Chen, *Chem. Eur. J.* **2011**, *17*, 7817–7822.
- [17] S. Bureekaew, H. Sato, R. Matsuda, Y. Kubota, R. Hirose, J. Kim, K. Kato, M. Takata, S. Kitagawa, *Angew. Chem.* **2010**, *122*, 7826–7830; *Angew. Chem. Int. Ed.* **2010**, *49*, 7660–7664.
- [18] a) F. Song, C. Wang, J. M. Falkowski, L. Ma, W. Lin, *J. Am. Chem. Soc.* **2010**, *132*, 15390–15398; b) B. Kesani, Y. Cui, M. R. Smith,

- E. W. Bittner, B. C. Bockrath, W. Lin, *Angew. Chem.* **2005**, *117*, 74–77; *Angew. Chem. Int. Ed.* **2005**, *44*, 72–75.
- [19] a) X. Lin, J. Jia, X. Zhao, K. M. Thomas, A. J. Blake, G. S. Walker, N. R. Champness, P. Hubberstey, M. Schröder, *Angew. Chem.* **2006**, *118*, 7518–7524; *Angew. Chem. Int. Ed.* **2006**, *45*, 7358–7364; b) X. Lin, I. Telepeni, A. J. Blake, A. Dailly, C. M. Brown, J. M. Simmons, M. Zoppi, G. S. Walker, K. M. Thomas, T. J. Mays, P. Hubberstey, N. R. Champness, M. Schröder, *J. Am. Chem. Soc.* **2009**, *131*, 2159–2171; c) S. Yang, X. Lin, A. J. Blake, G. S. Walker, P. Hubberstey, N. R. Champness, M. Schröder, *Nat. Chem.* **2009**, *1*, 487–493; d) Y. Yan, X. Lin, S. Yang, A. J. Blake, A. Dailly, N. R. Champness, P. Hubberstey, M. Schröder, *Chem. Commun.* **2009**, 1025–1027; e) Y. Yan, I. Telepeni, S. Yang, X. Lin, W. Kockelmann, A. Dailly, A. J. Blake, W. Lewis, G. S. Walker, D. R. Allan, S. A. Barnett, N. R. Champness, M. Schröder, *J. Am. Chem. Soc.* **2010**, *132*, 4092–4094; f) Y. Yan, S. Yang, A. J. Blake, W. Lewis, E. Poirier, S. A. Barnett, N. R. Champness, M. Schröder, *Chem. Commun.* **2011**, *47*, 9995–9997; g) L. Ma, D. J. Mihalcik, W. Lin, *J. Am. Chem. Soc.* **2009**, *131*, 4610–4612; h) S. Ma, D. Sun, J. M. Simmons, C. D. Collier, D. Yuan, H.-C. Zhou, *J. Am. Chem. Soc.* **2008**, *130*, 1012–1016; i) D. Zhao, D. Yuan, D. Sun, H.-C. Zhou, *J. Am. Chem. Soc.* **2009**, *131*, 9186–9188; j) D. Yuan, D. Zhao, D. Sun, H.-C. Zhou, *Angew. Chem.* **2010**, *122*, 5485–5489; *Angew. Chem. Int. Ed.* **2010**, *49*, 5357–5361; k) B. Chen, N. W. Ockwig, A. R. Millward, D. S. Contreras, O. M. Yaghi, *Angew. Chem.* **2005**, *117*, 4823–4827; *Angew. Chem. Int. Ed.* **2005**, *44*, 4745–4749; l) Y. Hu, S. Xiang, W. Zhang, Z. Zhang, L. Wang, J. Bai, B. Chen, *Chem. Commun.* **2009**, 7551–7553; m) Z. Guo, H. Wu, G. Sri-nivas, Y. Zhou, S. Xiang, Z. Chen, Y. Yang, W. Zhou, M. O'Keeffe, B. Chen, *Angew. Chem.* **2011**, *123*, 3236–3239; *Angew. Chem. Int. Ed.* **2011**, *50*, 3178–3181; n) O. K. Farha, A. Ö. Yazaydin, I. Eryazici, C. D. Malliakas, B. G. Hauser, M. G. Kanatzidis, S. T. Nguyen, R. Q. Snurr, J. T. Hupp, *Nat. Chem.* **2010**, *2*, 944–948.
- [20] Crystal data for **UTSA-33**: $C_{27}H_{25}N_2O_{10}Zn_2$; orthorhombic; space group *Pnma*; $a=25.9507(4)$, $b=25.7680(4)$, $c=10.5236(2)$ Å; $V=7037.1(2)$ Å³; $Z=8$; $D_{\text{calc}}=0.993$ g cm⁻³; $\mu=1.970$ mm⁻¹; $\text{GoF}=1.048$; $R_1(I>2\sigma(I))=0.0482$; wR_2 (all data)=0.1441.
- [21] a) M. O'Keeffe, M. A. Peskov, S. J. Ramsden, O. M. Yaghi, *Acc. Chem. Res.* **2008**, *41*, 1782–1789; b) M. O'Keeffe, M. Eddaoudi, H. Li, T. Reineke, O. M. Yaghi, *J. Solid State Chem.* **2000**, *152*, 3–20.
- [22] A. L. Myers, J. M. Prausnitz, *AIChE J.* **1965**, *11*, 121–127.
- [23] a) R. Krishna, S. Calero, B. Smit, *Chem. Eng. J. (Amsterdam, Neth.)* **2002**, *88*, 81–94; b) R. Krishna, J. M. v. Baten, *Chem. Eng. J. (Amsterdam, Neth.)* **2007**, *133*, 121–131; c) R. Krishna, J. M. v. Baten, *Phys. Chem. Chem. Phys.* **2011**, *13*, 10593–10616; d) R. Krishna, J. M. v. Baten, *J. Membr. Sci.* **2011**, *377*, 249–260.
- [24] J. A. Mason, K. Sumida, Z. R. Herm, R. Krishna, J. R. Long, *Energy Environ. Sci.* **2011**, *3*, 3030–3040.
- [25] R. Krishna, J. R. Long, *J. Phys. Chem. C* **2011**, *115*, 12941–12950.
- [26] G. M. Sheldrick, *SHELXS 97, Program for Crystal Structure Refinement*, University of Göttingen, Göttingen, Germany, **1997**.

Received: September 1, 2011

Published online: December 8, 2011